

Levitating Magnetic Insoles: A Novel Approach to Alleviating Plantar Fasciitis Through the Reduction and Redistribution of Plantar Pressures

Yue Yu¹

¹ Culver Academies, Culver, IN, United States

Correspondence: Yue Yu, Culver Academies, Culver, IN, United States.

doi:10.56397/JIMR/2024.09.04

Abstract

Plantar fasciitis, a leading cause of foot pain, affects a significant portion of the population, with an estimated prevalence of 10% during an individual's lifetime. This debilitating condition can result in substantial healthcare costs and decreased quality of life. The pain is attributed to the inflammation of the plantar fascia, which is crucial for supporting the foot's arch. Risk factors for plantar fasciitis include obesity, sedentary lifestyles, improper footwear, and biomechanical abnormalities. Current treatment options are primarily conservative, with varying levels of success.

In response, an affordable, lightweight, and soft, magnetic insole was developed as a novel approach to alleviate plantar fasciitis by reducing and redistributing plantar pressures with neodymium magnets. The final prototype achieves a magnetic repulsion force of approximately 84.57 lbs. and incorporates sensor modules to monitor data. The device also facilitates real-time data visualization between Arduino and personal devices, providing valuable insights into plantar pressure and walking characteristics for various patients.

Data analysis and structural optimization are further enhanced through the use of MATLAB and Excel, which generate heatmaps to visualize plantar pressure distribution. Future research should focus on increasing the magnetic intensity to improve pain relief effectiveness and incorporating personalized disease-specific adjustments to optimize the magnet placement within the sole. By addressing the prevalent issue of foot pain and offering a potential solution for plantar fasciitis, our levitating magnetic insoles demonstrate significant potential for enhancing the quality of life for a large portion of the population.

Keywords: magnetic suspension, plantar pressure, silicone casting, mathematic modeling, data visualization

1. Introduction

1.1 Background and Significance

American Podiatric Medical Association survey shows that four out of five Americans experience chronic foot pain (American Podiatric Medical Association, 2018). Usually, most people get inflammation of bones, ligaments, or tendons in the foot by overusing them in daily life. One of the most prevalent diseases is plantar fasciitis. It is the inflammation of a thick band of tissue that runs across the bottom of each foot and connects the heel bone to the toes (Mayo Foundation for Medical Education and Research, 2022). Flat feet are the leading cause of plantar fasciitis because the plantar fascia gets stretched away from the heel when bearing weight. Flatfeet are a common condition when the arches of the feet flatten out with pressure exerting on them. With flat feet, the entire soles of the feet will touch the floor. It is usually developed during childhood or later in life after an injury.

The primary goal of the project is to create an affordable, comfortable, and smart insole that uses magnetic levitation technology for pain relief biomedical device for patients with plantar fasciitis and incorporates sensor

modules to detect sole pressure and acceleration of every motion. The data will be used to analyze foot pressure distribution and further structural optimization.

1.2 Literature Review

Currently, the most prevalent device dealing with plantar fasciitis is the foot braces. By wearing foot braces, the patient can stretch the tendon and avoid sharp pain after waking up. However, this technique of relieving pain is relatively conservative and inconvenient to work with overnight.



Figure 1.1. Planter Fasciitis Foot Brace (DME for Less)

A similar pain relief equipment dealing with chronic pain is metatarsal (MT) pad. MT pads can have various forms and are made of numerous different materials. One type of material of MT pads is fabric.



Figure 1.2. Fabric Cushion MT Pad (Dr JK Ball of foot cushions – metatarsal pads, n.d.)

Figure 1.2 provides an example of MT pads made of fabric. Fabric metatarsal sleeve pads with forefoot cushion pad can prevent metatarsal ball pain and fracture through cushions with sole gel.

One potential disadvantage of MT pad is its equipped position, which can vary regions to regions on the foot. Therefore, researchers conducted experiments to determine the optimal position to place a MT pad with metatarsalgia patients. After obtaining the data of plantar pressure from 10 patients, researchers found that when patients walk without MT pads, the peak pressure was around 678 ± 227 in regions closer to heel called proximal. However, with the MT pad that causes the peak pressure of pad to encroach on region F, the pressure reduction is the most effective, and the mean proximal plantar pressure is reduced to 531 ± 144 kPa (Table 1.1). Therefore, the MT head reduces the most plantar when it is installed at a proximal position that has the largest pressure without the pad. (Wei-Li, H., Xin-Xian, L., & Jiunn-Horng, K, 2005) Similar research was also conducted, and researchers stated that the thickness of MT pads is a determinant factor in maximizing pressure reduction. The longitudinal axis location of the support, the deviation of the MT pad horizontally, was not a determining role in minimizing plantar pressure. (Brodtkorb, T.-H., Kogler, G. F., & Arndt, A, 2008)

Table 1.1. Peak Pressure Reduction Analysis (Brodtkorb, T.-H., Kogler, G. F., & Arndt, A, 2008)

Region	No Pad	Peak Pressure of Pad Encroached on F	Peak Pressure of Pad Encroached on E	Peak Pressure of Pad Encroached on D
--------	--------	--------------------------------------	--------------------------------------	--------------------------------------

A	491 ± 133	438 ± 149	359 ± 117	356 ± 147
B	637 ± 237	555 ± 166	433 ± 98	407 ± 151
C	687 ± 228	543 ± 129	431 ± 92	498 ± 93
D	678 ± 227	531 ± 144	427 ± 97	775 ± 217
E	615 ± 240	432 ± 98	570 ± 159	707 ± 178
F	454 ± 141	4555 ± 109	500 ± 112	557 ± 128

As a result of their strong magnetic field properties, Neodymium magnets are used in a variety of modern technologies, as well as in medicine. Neodymium magnets also can provide similar pressure reduction properties as soft gels. Recent research has also shown that this type of magnet appears to hold great promise for both diagnostic and therapeutic purposes. More specifically, evidence has supported that the Neodymium magnets do not have any adverse effect on an individual’s skeleton, muscle, or joints system (Yaghoubi, H, 2012).

In fact, as early as 2000, Weng-Pin Chen, Fuk-Tan Tang, and other engineers have conducted research regarding the force distribution during different walking stage by 3D analysis. The researchers constructed a model following male patient foot anatomy and built a 3D model to evaluate the walking dynamics of the foot. The study created a preliminary computational model that was able to estimate the overall plantar pressure and bone stress distribution (Chen, W. P., Tang, F. T., & Ju, C. W, 2001). In the experiment, the researchers found that the plantar pressure falls in between the range of “374 to 1003 kPa.”

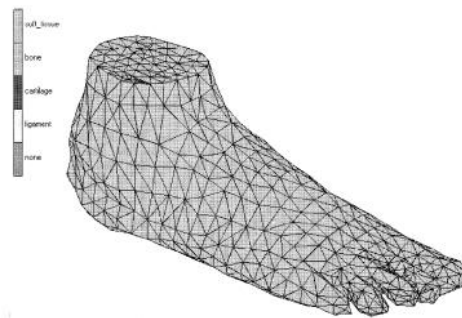


Figure 1.3. Constructed 3D model (Chen, W. P., Tang, F. T., & Ju, C. W, 2001)

In 2007, S. Butdee invented a breaking new way to design sport shoe soles. The new hybrid between solid and surface modeling. The design allowed the user to modify the specifics of the sole to ensure sole customization. The digital model also promoted the design efficiency of the sole by allowing sole personalization and a more comfortable sport shoe sole (Butdee, S, 2002).

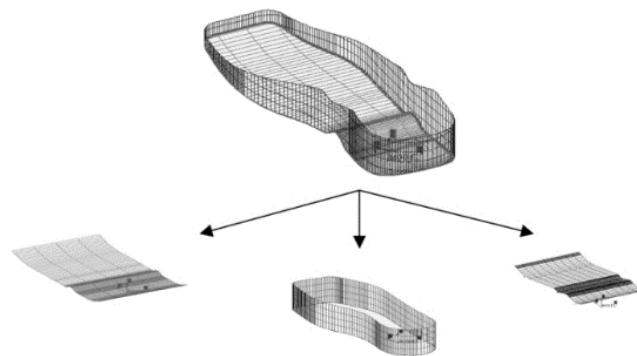


Figure 1.4. Hybrid Sole Design (Butdee, S, 2002)

Butdee was not the only researcher in the realm of sole customization. In 2019, Davide Jose, Troy Nachtigall, and others started their study on personalized shoe sole design using meta-material. Their study showed that through computational algorithms and modeling, people are able to construct highly customized soles based on individual

foot features (Amorim, D. J. N., Nachtigall, T., & Alonso, M. B., 2019). Combined with software, the meta-material they used are able to produce a shoe sole with different characteristics and stiffness, corresponding to the user's personalization traits.



Figure 1.5. Personalized Sole (Amorim, D. J. N., Nachtigall, T., & Alonso, M. B., 2019)

Sole customization was also not limited in sport shoes. In 2007, Jia Yu, Yubo Fan, and multiple others innovated new model of female foot for the design of high-heeled shoes. The researchers developed 3D anatomical detailed FE models of the female foot, ankle, and its high-heeled supports. With the model, the study explored the plantar contact pressure and internal load response of plantar bone and soft tissue structures. The experiment also included a variety of heel heights during simulation (Yu, J., et al, 2008).

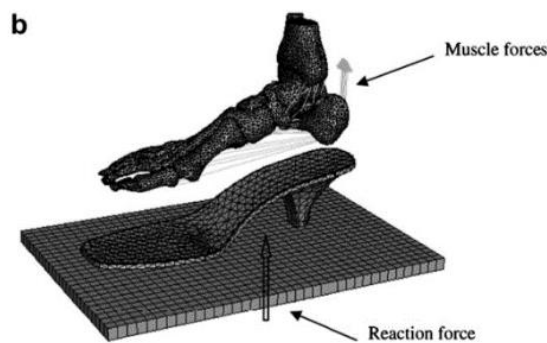


Figure 1.6. Loading conditions with high-heeled shoes (Yu, J., et al, 2008)

Regarding the application of magnetic forces in shoe design, in 2020, researchers following Muhammad Iqbal completed study on electromagnetic insole energy generator. Iqbal invented a hybrid insole energy collector (HIEH) that collects energy from low-frequency walking step motion to power a wearable sensor. The device makes converting energy from walking step to electrical power possible and utilizes the generated electricity as the power source of the wearable sensor (Iqbal, M., et al, 2020).

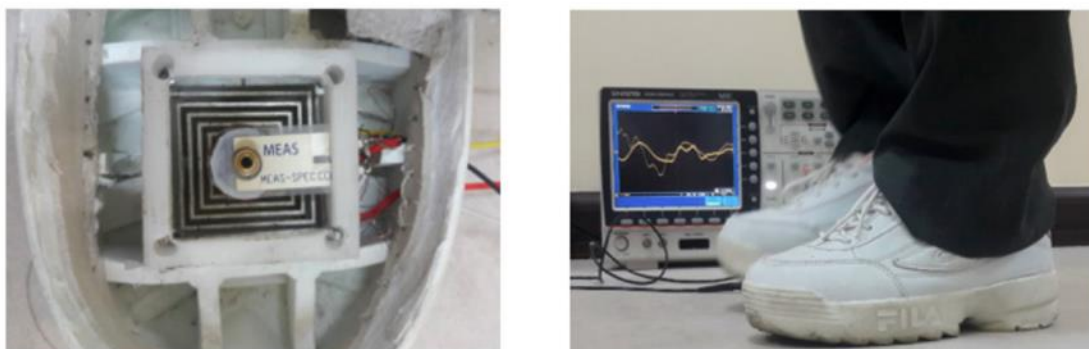


Figure 1.7. Wearable HIEH and sensor (Iqbal, M., et al, 2020)

Quasi-static simulation was also completed by a group of researchers in 2015. By using a 3D finite element analysis, researchers were able to construct a model of foot composed of bones, cartilage, ligaments, and a complex-shaped plantar fascia. With the constructed model, people are able to simulate the mechanical structure and tensions existing in the foot and put forth well-designed shoes that foster better walking experience and less pain (Chen, Y. N., et al, 2014). The research also had enormous potential clinical application.

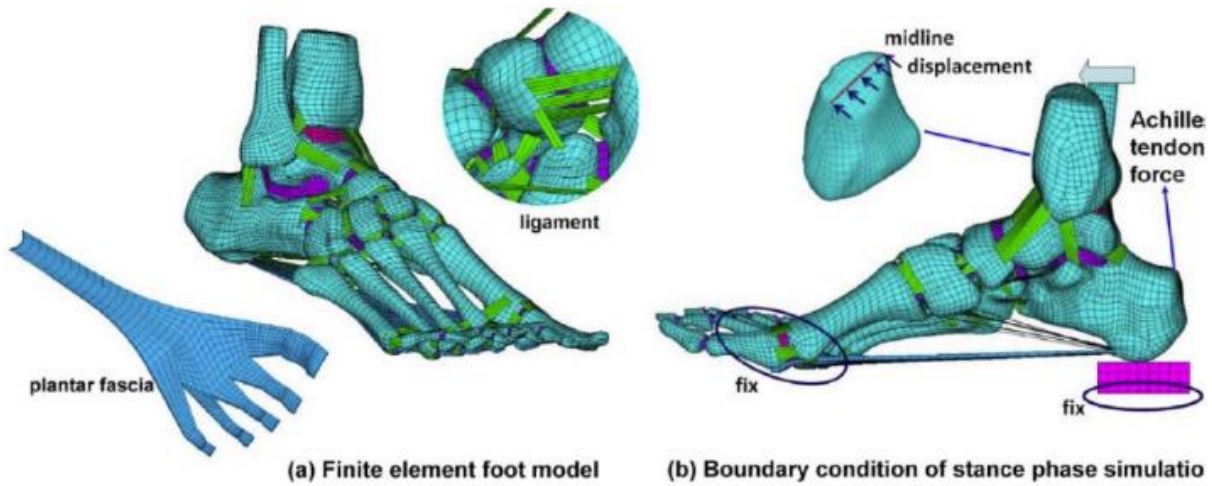


Figure 1.8. Finite Element Foot Model (Chen, Y. N., et al, 2014)

The report is organized as follows. Engineering Design describes the development of my prototypes and the features of my final version of the device. Experiments details the experiments that I conducted to optimize my design and the results and discussions of the experiments. Results interprets the data I acquire from the experiment. Conclusion summaries and states the determining finding of the paper.

2. Theoretical Design

Magnets are objects made up of iron, cobalt, and nickel. Magnets generate magnetic fields and attract ferromagnetic materials such as iron, nickel, cobalt and other metals. Magnet is divided into permanent magnet and electromagnets. The most prominent magnet is artificial Neodymium magnets, which is so far the strongest permanent magnetic. Its chemical formula is Nd₂Fe₁₄B. Due to their physical properties, magnets are able to generate magnetic fields that allow attraction and repulsion with each other.

We can estimate the repulsion force of the magnet using the K&J magnetics website. Using the most common type of magnetic grade, N42, the estimated repulsion force between two discs of 20 mm in diameter and 2 mm in thick is 5.59 lbs. when two magnets adhered to each other (K&J Magnetics – Repelling Magnet Calculator, n.d.). As Figure 2.1 shows, the amount of force decreases exponentially as the distance in between increases.

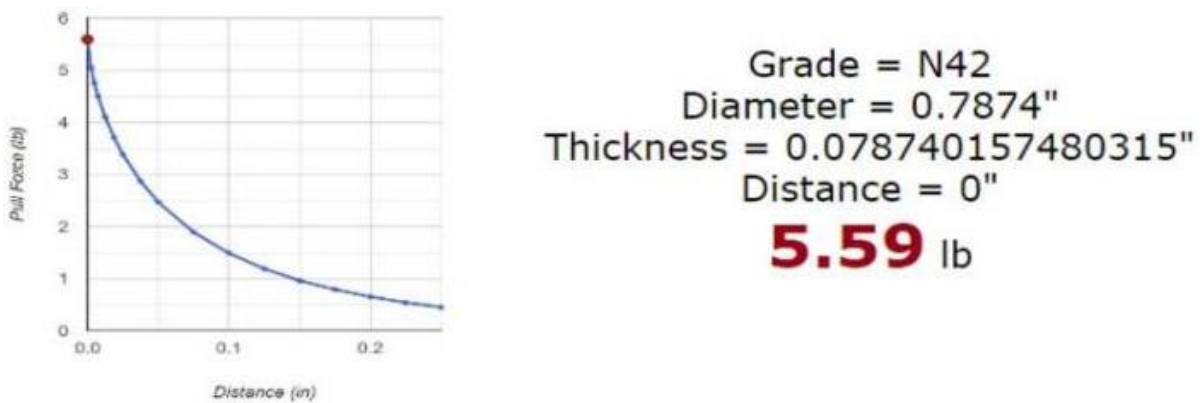


Figure 2.1. Estimated Repulsion Force (K&J Magnetics – Repelling Magnet Calculator, n.d.)

With the addition of magnetic repulsion during the walking phase, patients with chronic foot pain can receive less tension at the metatarsal and calcaneus regions. Moreover, the pressure distribution should be able to minimize the tension pressed on the collateral ligaments and require less tendon force exertion.

The initial design is conceptualized based on the foot model of my foot. The print of my foot was transcribed on a piece of paper and was then constructed in SolidWorks software. The outline of the prototype was also constructed in a way so that the foot pressure sensor RX-ES40-48P can fit perfectly into the two sides of the model and leave enough space for screws and bolts. Therefore, the size of the model is approximately 100mm, its height being about 265mm. The holes reserved for bolts are also designed to avoid the wires from the RX-ES40-48P sensor.

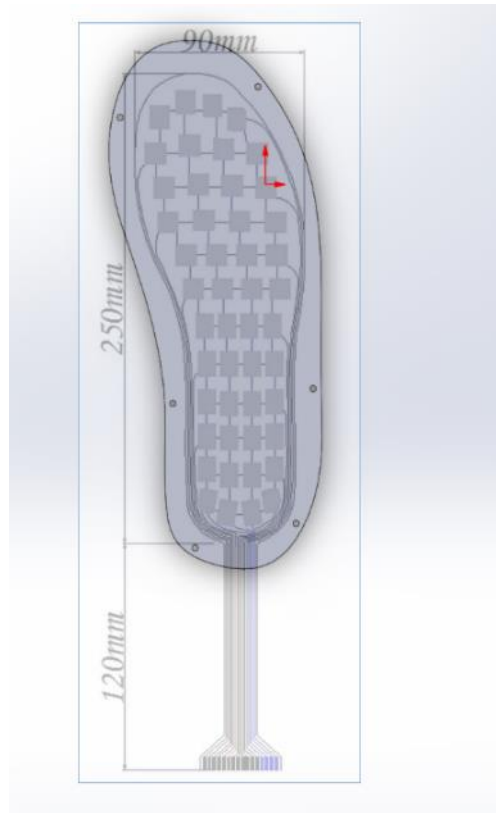


Figure 2.2. Transcription of the Sensor to 3D Model

3. Structural Design

In the first iteration of the device, the device's structure is constructed with wooden plates. The sole was formed with four laser cut wooden plates. Each of the two wooden plates form the top and bottom section with the 25mm diameter and 2mm thick Neodymium magnets placed in one of the carved wooden plates. The carved plate faces inside so that it prevents the magnets displacing from each other due to the repulsion force. The boards also thus hold the sole together withstanding the weight of an individual's foot with bolts. Since the connection between the boards is bolts, it is required to reserve holes for the nuts in order to close the two boards together fully to ensure the accuracy of the measured pressure data. Therefore, a circle of 6.1mm in diameter is cut out on the according space for the nut, allowing the complete shut of the two wooden boards.

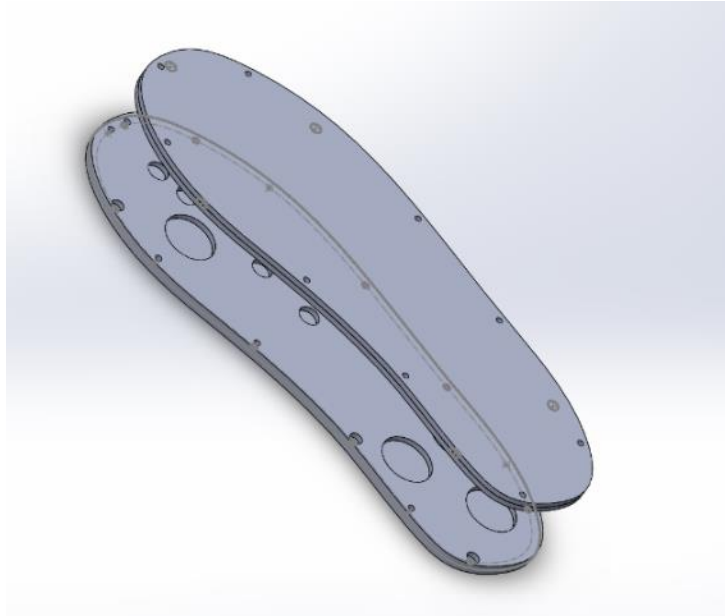


Figure 3.1. The assembly of the 3D modeled prototype

Using the K&J website, we can find the approximate repulsion force in the prototype sole. When two 25mm diameter, 2mm thick discs touch each other, the repulsion between them is about 7.35 lbs. After the device is equipped by the user, the maximum repulsion force occurs during the standing phase when all 7 pairs of magnets are the closest to their corresponding magnets. There are also 8 pairs of 10 mm diameter magnetics to further improve the repulsion, which is about 2.38 lbs each. Eventually, the repulsion is approximately $7 * 7.35 \text{ lbs} + 8 * 2.38 \text{ lbs} = 70.49 \text{ lbs}$. With this amount of force, the plantar pressure accumulates at the calcaneus and metatarsal region.

However, since the bolt connecting two plates are unable to be fully hidden when the two sections are closed together, there is always a segment of the bolt leaving outside of the device, which might cause injury or discomfort of the user. Therefore, other iterations of the sole were attempted to find the optimal.



Figure 3.2. Built wooden board device

The final design of the device is developed to have four parts: the silicone gel with embedded Neodymium magnets, data detection module, data transmission module, and an outer portable shell. The silicone was constructed through 3D modeling. In my prototype, Neodymium magnets were embedded in two separate silicon gels in opposite

polarity, formed in laser-cutting molds. Two separate pieces of gel are connected by three rubber bands. The data detection module is comprised of a pressure sensor and a motion detector. The pressure sensor module in between two gels then collect pressure data of each step taken by the user, and the motion detector is attached to the outer shell detecting the acceleration and movement of each step taken by the user. The transmission system is used to transport data obtained from the pressure sensor and the motion detector to a mobile device through Bluetooth transmission, allowing the individual to know the information the steps they took. Along with pressure sensor, a multipurpose sensor that is able to detect temperature, acceleration, deviation is also attached to the outer shell, sending real-time information to the mobile device.

3.1 Silicone Gel Casting

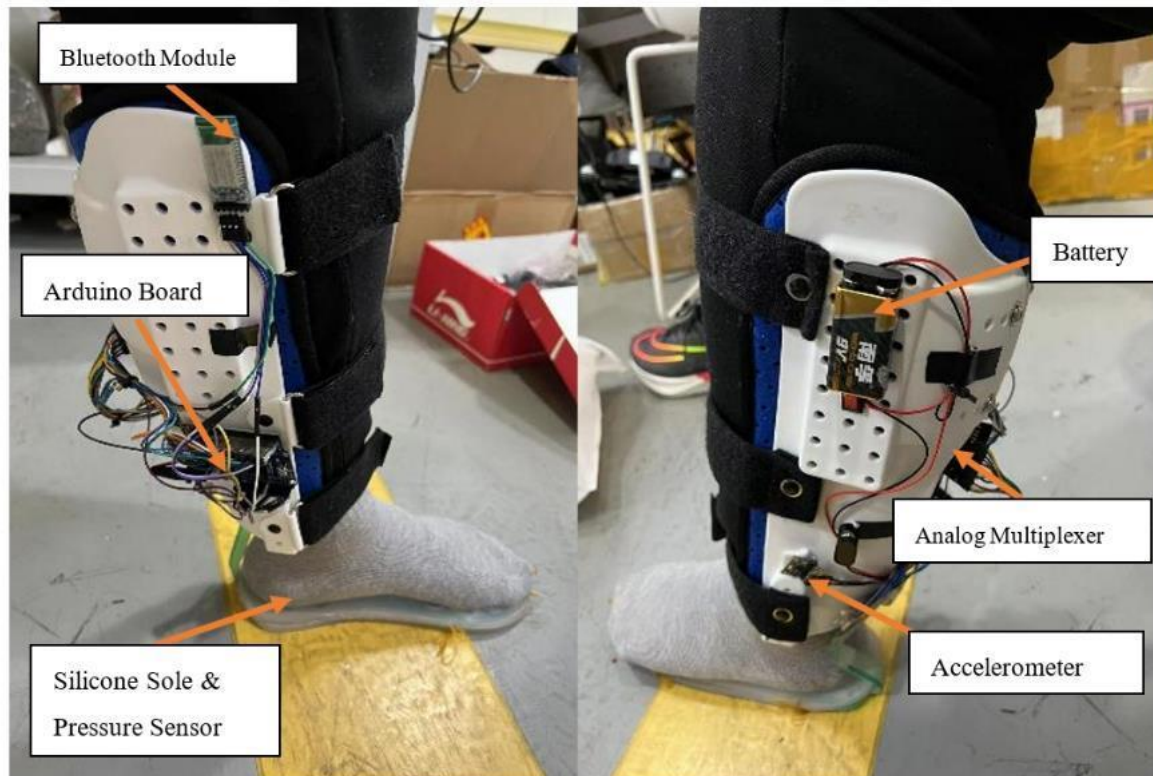


Figure 3.3. Final Prototype

The gel is a type of two-component AB gel, which is composed of two parts, the glue, and the hardener. The gel needs to be evenly mixed according to a certain 1:1 proportion, and then can be used for casting. Two-component liquid silicone AB gel can be cured at room temperature. Moreover, to prevent the further foaming of the gel, the mixed gel is first placed into a vacuum chamber to eliminate any possible air bubbles. To accelerate the process of curing, the gel might also be placed in the oven.

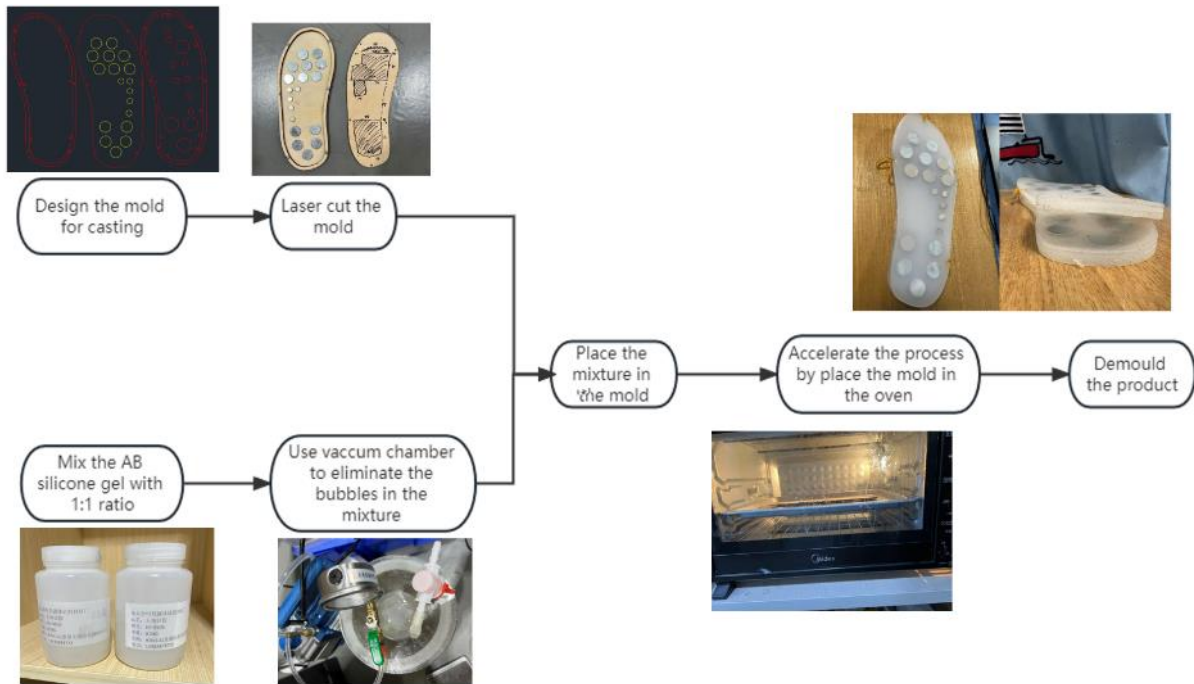


Figure 3.4. Casting Procedure

The formation of the sole is done by two separate castings. The first-time casting created half of the sole. Next, the magnets are placed into designed positions. Then, the second half of the sole is cast following the same process. Using AB silicone gel as the material of the sole has two benefits. The gel strongly holds the magnets in place, preventing any potential displacement of the magnet due to strong magnetic repulsion. In addition, it gives a softer and more flexible texture than wooden boards, which can give the sensor a more accurate pressure data.

3.2 Outer Shell

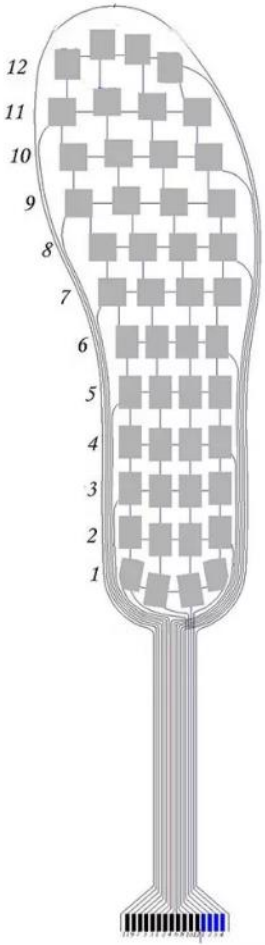
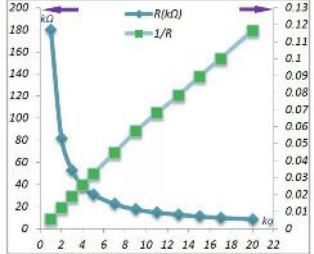
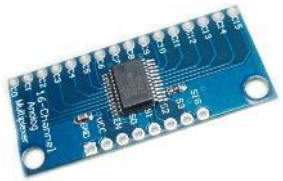
The outer shell is modified based on a current product of calf bone fracturing attaching clamp. The product allows me to produce a portable device with all the functional parts. The outer shell has soft inner layer that can make the user have a comfortable using experience and a plastic, hard outer shell to allow the installation of Arduino boards and other necessary circuits, sensors and power source.



Figure 3.5. Attaching Clamp

4. Electronics Design

4.1 Electronics Component

Name	Picture	Details	Purpose
<p>Arduino main board</p>		<p>Working voltage 5V Input voltage 9V</p>	<p>Part of the Control circuit. Installed outer shell of the device. Through the programmed language, converting signal to high or low frequency output to different circuit elements, the components in the circuit to control components.</p>
<p>RX-ES40-48P Plantar Pressure Sensor</p>		<p>Working voltage 5V 250mm length 12 by 4 pressure sensor matrix Produce different analog output under different pressure. The higher the pressure, the higher analog output.</p> 	<p>Part of the detection circuit. Installed between the sole of the device. Converting pressure and weight distribution to analog input to the Arduino Board. As weight increases, the analog output increases.</p>
<p>CD74HC4067 16 Channel Analog Multiplexer</p>		<p>Working voltage 5V 16 analog channel input Expand the analog pin of the Arduino board and allow the measure of the pressure sensor.</p>	<p>Part of the detection circuit. Connect directly to the pressure sensor. Connect to the 16 output pins of the pressure sensor and measure each of the pressure in an iteration pattern.</p>

<p>MPU6050 Accelerometer and Gyroscope Sensor</p>		<p>Working voltage 5V Temperature, acceleration, position, deviation detection</p>	<p>Part of the detection circuit. Able to detect detailed information for each movement of the user.</p>
<p>HC-05 Bluetooth Module</p>		<p>Working voltage 5V Transmits data from Arduino board to other connected devices, such as phones or Arduino.</p>	<p>Part of the transmission system. Connect the Arduino Board with mobile phone devices to fulfill real-time data transmission.</p>

4.2 Detection Module

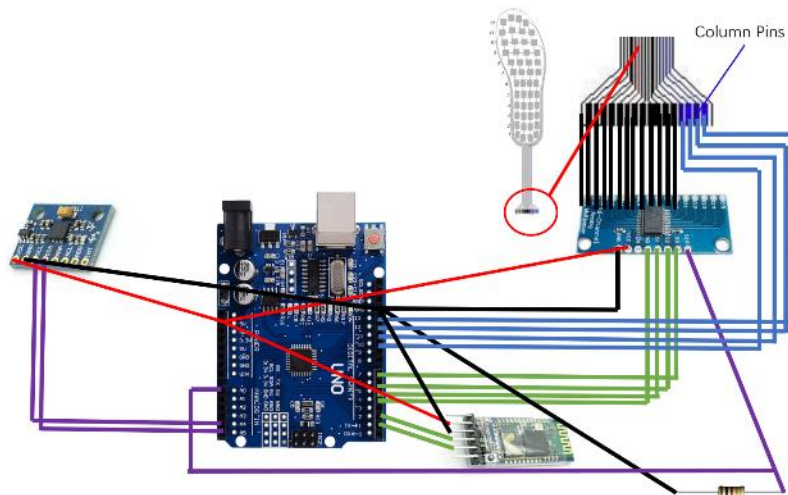


Figure 4.1. Circuit Connection

The device's electric is separated into three modules: pressure sensor module, Bluetooth module, and the multipurpose Accelerometer and Gyroscope module.

The detection circuit of the pressure sensor is composed of a 10k ohm resistor, a Rx pressure sensor, and analog output of the Arduino board. The Rx pressure sensor is basically a varying resistor. The amount of mass on the sensor is negatively proportional to the amount of ohm the resistor exhibits. Therefore, in order to obtain the amount of mass on the sensor, calculations and conversions are required.

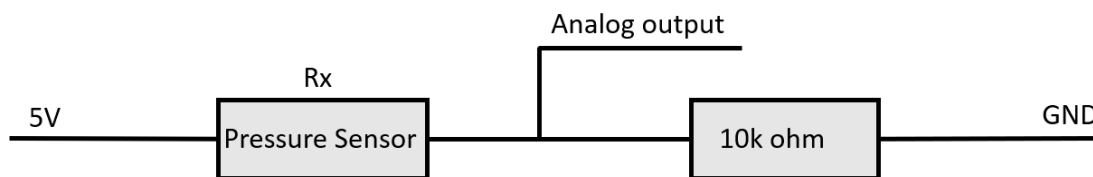


Figure 4.2. Relation of the pressure sensor between resistance and mass (Changzhou Rouxi Electronic Technology Company, n.d.)

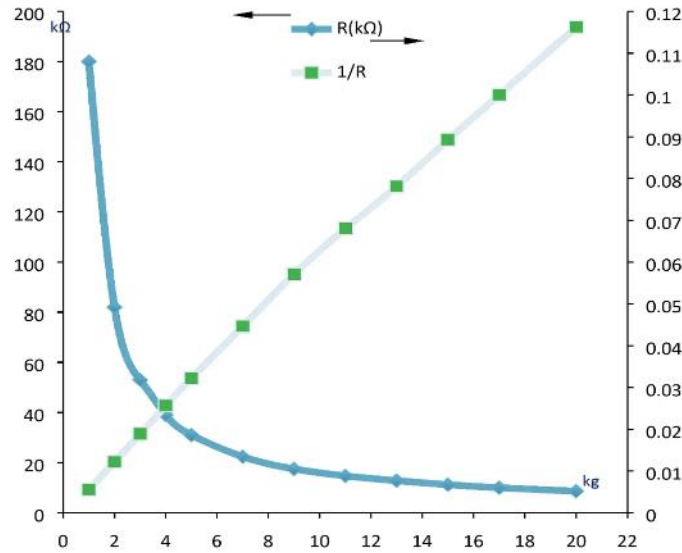


Figure 4.3. Detection Circuit of the Pressure Sensor

m: mass

Rx: the resistance exhibited by the pressure sensor

u: voltage detected by the analog output

x: analog value

We know that the Arduino analog input ranges from 0 to 1023, representing the voltage from 0 to 5 volt. Therefore, using the analog value x, we can find the voltage: $u = 5V \frac{x}{1023}$

$$m = a \frac{1}{Rx}$$

$$a \approx 20 * 0.118 \approx 169.5$$

According to the formula of voltage division, we know that the voltage measured by A0 is $u = \frac{10k\Omega}{Rx+10k\Omega} \times 5V$

$$\begin{cases} u = \frac{10k\Omega}{Rx + 10k\Omega} \times 5V \\ m = \frac{0.0059}{Rx} \end{cases}$$

$$uRx + 10k\Omega u = 10k\Omega \times 5V$$

$$uRx = 10k\Omega \times 5V - 10k\Omega u$$

$$Rx = \frac{10k\Omega \times 5V - 10k\Omega u}{u}$$

$$m = \frac{169.5 u}{10k\Omega \times 5V - 10k\Omega u}$$

$$m = \frac{169.5 \times 5V \frac{x}{1023}}{10k\Omega \times 5V - 10k\Omega \times 5V \frac{x}{1023}}$$

$$m = \frac{169.5 \times \frac{x}{1023}}{10k\Omega \left(1 - \frac{x}{1023}\right)}$$

$$m = \frac{169.5 x}{10\Omega(1023 - x)}$$

Therefore, we are able to convert the voltage output from the Arduino Serial Monitor into specific mass output during the measurement process of the pressure sensor.

The pressure sensor's data is obtained by Arduino through the multiplexer. The pressure sensor has 48 small sensors embedded in it. The entire sensor has 16 pins, 12 row pins, and 4 column pins. When we need to test the pressure on a certain sensor, only the corresponding column pin needs be activated using high voltage, and the multiplexer's channel will be adjusted to the corresponding row pin in order to receive the right analog output. For example, when we need to test the sensor on row 1 column 1, we first need to inactivate all the column pins and only active the column 1 pin. Then we need to turn the multiplexer to receive the data from row 1. Finally, we will be able to receive analogy values from Arduino.

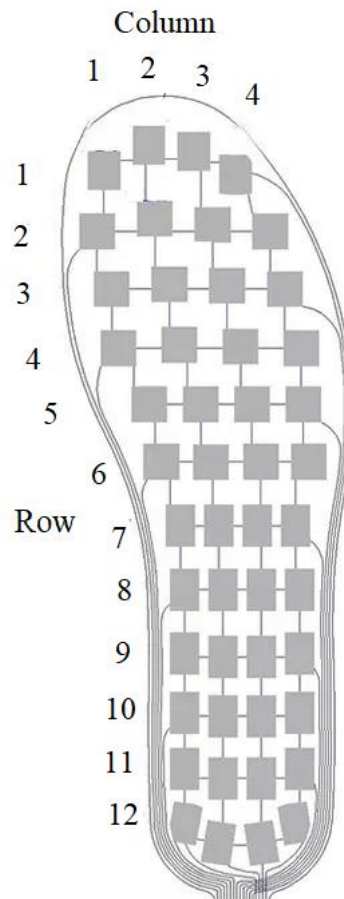


Figure 4.4. Pressure sensor layout (Changzhou Rouxi Electronic Technology Company, n.d.)

MPU6050 Accelerometer and Gyroscope Sensor is the other sensor the device is equipped with. The device is able to detect acceleration, position, and deviation detection. In Arduino program, a public library, MPU6050_tockn, is used for the data acquire and collection.

The control of the device is fulfilled through the Arduino board and the program uploaded. When the device is activated, the 9V battery powers the Arduino board and starts different modules attached to Arduino. The sensor modules, pressure sensor and accelerometer, are activated. Then, after the data is measured, Arduino transferred them to Bluetooth module that is able to real-time update the data to mobile phone application and, through Serial Monitor, to the MATLAB application on the computer to fulfill data visualization. The following is the logic map of the device:

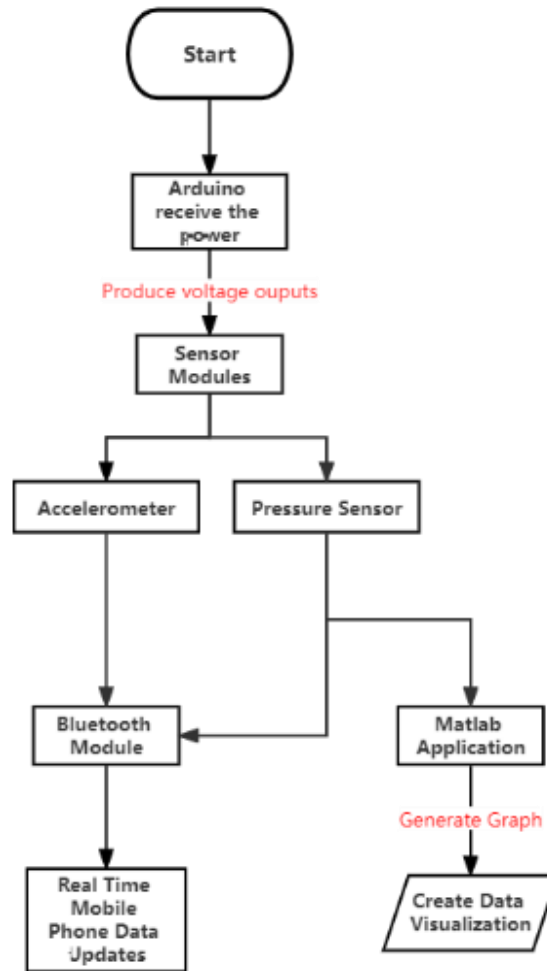


Figure 4.5. Control Circuit Flow Chart

4.3 Bluetooth Module

The Bluetooth module is connected to the Arduino board of the device. After the acquisition of data from pressure sensor and accelerometer, the Bluetooth module is able to transfer the data to mobile phone application, blinker, which allows the real-time update of data.

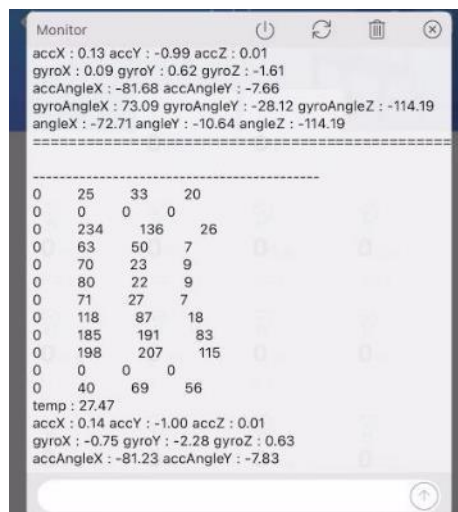


Figure 4.6. Mobile Phone Real-time data

4.4 Data Visualization

The MATLAB application allows the visualization of data through the Serial communication between Arduino and MATLAB. The design of the application is separated to interface and program design. The interface is designed as follows:

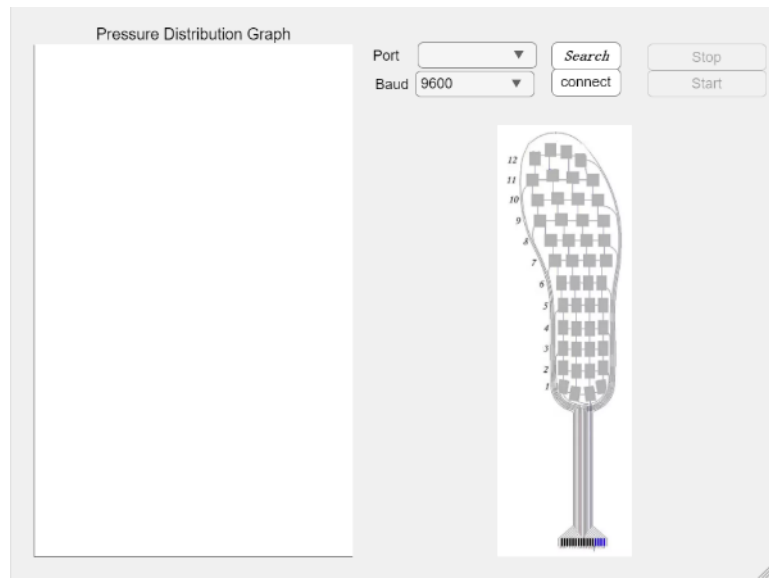


Figure 4.7. MATLAB App Interface

The upper right corner has four buttons and two dropdown menus. It allows the search and connection to Arduino Serial Monitor, which is required before receiving data from Arduino. The lower right has an image of the pressure sensor, which can act as a reference to aid the data analysis. On the left side of the scene is UI Axes, which would be the major data visualization area.

In the program design, the communication between Arduino and MATLAB is completed through the function embedded in the search and connect button. When the search button is pressed, the items in the port dropdown box is changed to available ports.

```
app.PortDropDown.Items=serialportlist("available");
```

Then, when the correct port and baud rate is selected, the connect button can be pressed. After the application first deletes any preexisting connection between the port to the application, which ensures the stable connection, a communication will be created between Arduino and the application.

```
com=app.PortDropDown.Value;
delete(instrfind({'Port'},com));
baud=str2double(app.BaudDropDown.Value);
app.S= serialport(com,baud,'Timeout',5);
fopen(app.S);
```

Afterwards, the start button is enabled. There is a function created in the callback function of the start button. When Arduino communication has any information, the application reads and records data and changes it into the format of string.

```
if app.S.NumBytesAvailable>0
    str=readline(app.S);
    str = deblank(str);
    str2= regexp(str, ',', 'split');
```

Finally, it transfers string data to number and places it into a 1 X 4 array. When the 1 X 4 array is filled, it then places the data in this array into a larger all data array.

```
len=length(str2);
```

```

Alldata=[];
lendata=[0 0 0 0];
for i=1:len
    if mod(i,4)==0
        lendata(4)=str2double(str2(i));
        Alldata=[Alldata;lendata];
    end
    if mod(i,4)~=0
        lendata(mod(i,4))=str2double(str2(i));
    end
end

```

After data transcription, the data is visualized in the UI Axes through the following function.

```
imagesc (app.UIAxes,Alldata)
```

The following is the data visualization produced by the application:

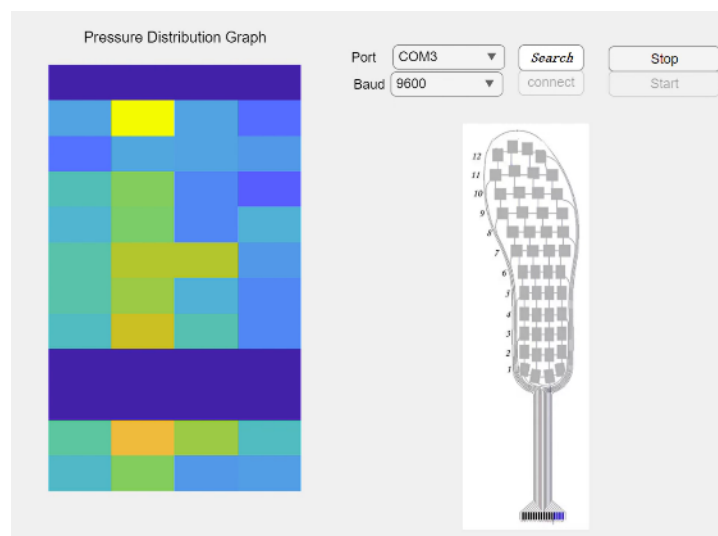


Figure 4.8. Data Visualization

5. Experiment

The experiment section is separated into two different experiments, the stationary and the shock absorbance test. The stationary experiment evaluates the prototype's ability to distribute pressure and weight when the patient is in a standing position. The shock absorbance test measures the specific amount of force experienced over a normal step.

5.1 Stationary Experiment

5.1.1 Experimental Design

The experiment will be completed on myself to determine whether the device helps with the distribution of sole pressure in the standing motion. In the experiment, the independent variable is the usage of magnetic levitation in the device, the dependent variable is the pressure analog output from the Serial monitor, and the control variable is the person using the device and the actions doing after wearing the device. The control group in the experiment for comparison is the silicone sole created without any magnet installed. Both devices, one with the installed magnet and the other not, will be separately tested. The data will be recorded after equipping the device and normally standing barefoot.

The following is the detailed step of the experiment:

- 1) Equipped the prototype
- 2) Connect the prototype with computer and open the Serial Monitor

- 3) Stand on the prototype
- 4) Record the analog value from the Serial Monitor
- 5) Repeat step 2-5 after equipping with device without any embedded magnet.

5.1.2 Data Selection

The data will be collected in the form of string through a serial monitor in the Arduino application and more detailedly analyzed in Excel. The data is created by the acceleration and pressure sensors evaluating the pressure data from the prototype shoe pad. The obtained data will help me analyze magnetics' effectiveness in helping the distribution of sole forces. The data will be compared to the data obtained from the control group, the device without the installation of magnets, to evaluate the extent of magnet levitation force helping the distribution of foot pressure.

The data is collected in the form of 12 by 4 tables with values representing the amount of force on the pressure sensor. The table is transported to excel to be analyzed by using different colors, with green being the lowest pressure and red being the highest pressure.

The control is experimented on silicone gel with the same hardness. Data with the total mass between 65 and 70 kg and centered are selected. The amount of weight applied on the device is calculated through the derived formula:

$$m = \frac{169.5 x}{10\Omega(1023 - x)}$$

After the calculation, all mass values from 48 sensors are summed together to find the total weight on the pressure sensor, which determines whether the data is valid or not. Due to the susceptibility of body mass deviation, the data sample that has a mass lower than 65 kg or higher than 70 kg are eliminated. Moreover, it is possible for people to have a slanted foot touching the ground. Therefore, all the data points in the selected sample need to be centered, meaning the greatest value and pressure need to be in the middle two columns of the graph.

5.1.3 Data Analysis

Table 5.1. Pressure data from Prototype (Standing)

12	6	18	17
5	0	20	7
55	110	118	77
45	124	126	112
18	53	77	56
9	7	0	0
3	11	0	0
5	0	0	0
2	9	18	2
9	48	126	129
16	135	144	226
23	164	212	176

Table 5.2. Control group

40.5	79.0	10.7	127.3
0.2	17.8	0.0	2.7
55.8	180.3	125.5	48.2
61.5	161.1	133.8	43.5
64.7	66.8	32.8	14.4
80.9	59.3	0.0	0.0
76.2	50.9	0.0	0.0
80.0	70.2	5.5	0.0

68.3	103.3	84.0	39.2
70.5	152.8	150.0	119.1
90.8	163.1	186.0	165.0
94.8	161.3	185.8	158.7

Therefore, it is clear that the control group has more concentrated pressure in the metatarsal and heel region of the foot. Moreover, the prototype group showed a less area of 0 weight sensors, showing that some weights were distributed to the section.

5.1.4 Pain Threshold

After understanding that the prototype is effective in optimizing the pressure distribution for a normal person, it is still important to find the connection between the pressure and the pain relief. According to the research by Yunqi Tang and few others (Tang, Y., et al., 2020), for a health man, the threshold value for discomfort is at 483 kPa for medial metatarsal, 291 kPa for the great toe, and 888 kPa for the heel region. With calculation, the maximum pressure at the medial metatarsal, the great toe, and the heel region are 371 kPa, 272 kPa, 317 kPa respectively. All values are lower than the discomfort threshold value. The conversion is completed through the equation: kPa value = kg/cm² value x 98.0665.

Table 5.3. Sample group in kPa

0	9.294597	40.61256	272.0937205
71.89	118.9165	14.24621	0
94.549008	371.2066	216.2317	110.8353409
80.118635	180.1908	170.7976	172.0718378
69.480634	67.44558	52.27327	3.702807189
37.59423	49.02494	0	0.335796008
53.540514	27.9167	0	0
67.630349	54.62852	36.17829	0
85.780819	163.1964	181.0504	55.17314483
92.06038	262.0362	266.5708	122.8906105
120.30507	263.2271	316.6359	226.8707434
115.94982	243.6805	290.6109	201.0869636

5.2 Shock Absorbance Experiment

5.2.1 Experimental Design

The experiment of shock absorbance is completed similar to the stationary experiment. The independent, dependent, and control variables remain the same for the test. The most noticeable change, however, is the data collection process was conducted when the test subject is walking.

The following is the detailed step of the experiment:

- 1) Equipped the prototype
- 2) Connect the prototype with computer and open the Serial Monitor
- 3) Walk normally with the equipped prototype
- 4) Record the analog value from the Serial Monitor
- 5) Repeat step 2-5 after equipping the sole without magnets

5.2.2 Data Selection

The experiment data is collected over the process of normal walking. Therefore, the data must show a specific pattern of pressure distribution. The pressure will be focused on the heel, then shift to the ball of the foot, eventually receding, shown in Figure 5.1. Therefore, only data points conform to this specific pattern will be selected. The formatting of the data also needs to be considered due to large volume of testing data. To ensure the best accuracy

of the analysis, the data is grouped together from zero value to zero value, ensuring that each step the subject took is a separate group.

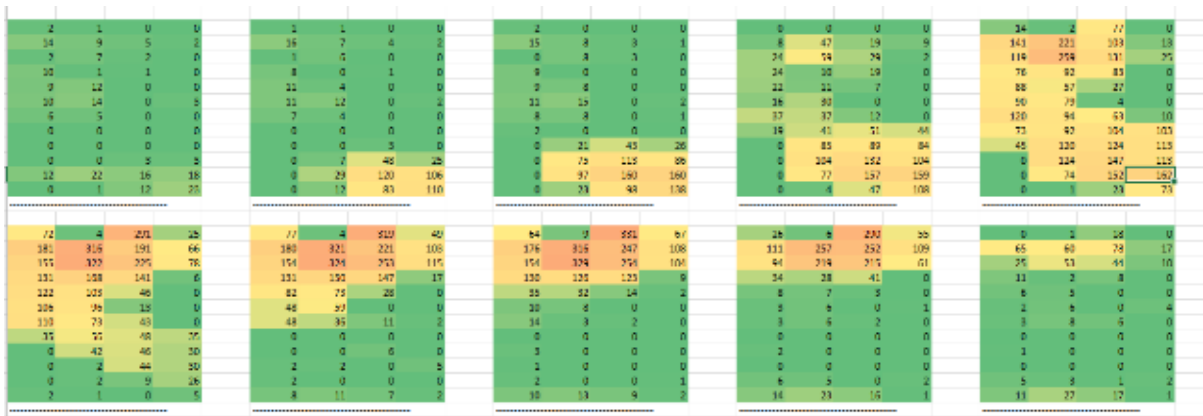


Figure 5.1. Sample sequence of pressure distribution during a normal step

5.2.3 Data Modeling

The analysis is then conducted in Excel after finding the mean of heel and the metatarsal pressure over each step. The graph is then generated for both prototype and control group.

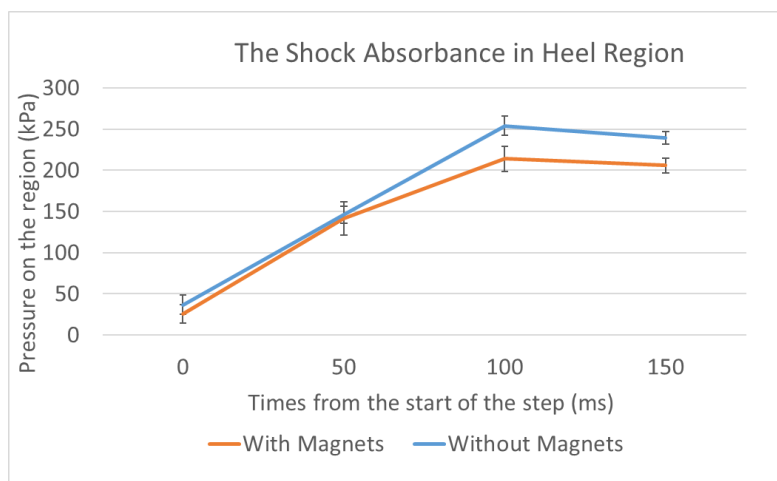


Figure 5.2. Shock Absorbance in heel

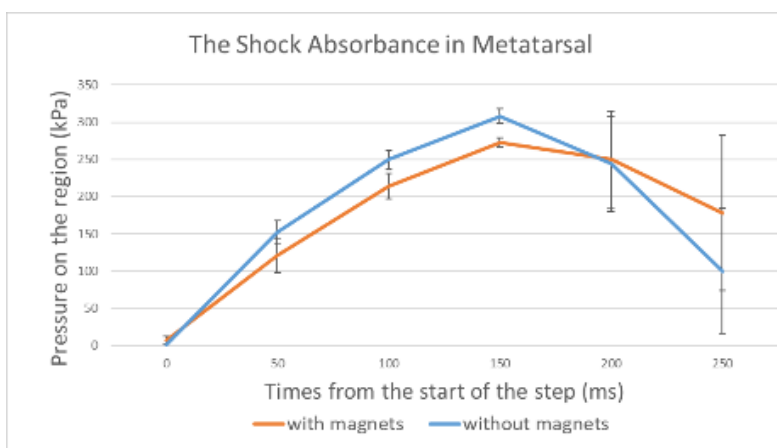


Figure 5.3. Shock Absorbance in metatarsal

The graph above clearly showed the trend that the prototype shows a better ability in absorb shock and distribute it evenly throughout the sole. The data groups on the peak for both graphs show that the control group without magnets show approximately 50 kPa more pressure than the prototype, suggesting the pressure reduction ability possessed by the device. Moreover, not only all values are significantly below discomfort level, but there is also a 16% pressure decrease on heel and a 12% pressure decrease on metatarsal.

6. Conclusion

The project partially completed the objectives. With the help of neodymium magnets, the device can help the plantar pressure distribution to a minor degree. The project also fulfills the real-time data transmission and visualization between Arduino and personal devices, which produces valuable data to analyze plantar pressure and walking characteristics of different patients.

7. Future Work

To expand on the study, it would also be valuable to strengthen the intensity of the magnets and promote the effectiveness of pain relief. It will also be essential to include the personalization of the device by creating 3D models based on patients with different foot diseases and chronic pain, which will optimize the pain relief for individuals. Finally, it is also important to include actual patients in the experiment, which should significantly improve the reliability of the device and determine its effectiveness on different individuals.

Reference

- Acharya, K., & Ghoshal, D. (2018). Animation of Magnetically Levitated Shoes and Its Optical Flow with Computer Vision. *International Journal of Engineering and Manufacturing*, 8(3), 40–53. <https://doi.org/10.5815/ijem.2018.03.04>
- American Podiatric Medical Association, (2018, October). The American Podiatric Medical Association 2018 Podiatric Practice Survey Findings Report. https://apma.cms-plus.com/files/2018%20Practice%20Survey%20Results_FINAL.pdf
- Amorim, D. J. N., Nachtigall, T., & Alonso, M. B. (2019). Exploring mechanical meta-material structures through personalised shoe sole design. *Proceedings of the ACM Symposium on Computational Fabrication*. <https://doi.org/10.1145/3328939.3329001>
- Benhama, A., Williamson, A. C., & Reece, A. B. J. (2000, November 1). A virtual work approach to the computation of magnetic force distribution from Finite Element Field Solutions. *IEE Proceedings — Electric Power Applications*. <https://doi.org/10.1049/ip-epa:20000724>
- Brodtkorb, T.-H., Kogler, G. F., & Arndt, A. (2008). The influence of metatarsal support height and longitudinal axis position on plantar foot loading. *Clinical Biomechanics*, 23(5). <https://doi.org/10.1016/j.clinbiomech.2007.09.019>
- Butdee, S. (2002). Hybrid feature modeling for sport shoe sole design. *Computers & Industrial Engineering*, 42(2-4), 271–279. [https://doi.org/10.1016/s0360-8352\(02\)00046-3](https://doi.org/10.1016/s0360-8352(02)00046-3)
- Changzhou Rouxi Electronic Technology Company, (n.d.). RX-ES-48P pressure sensor. Taobao.
- Chen, W. P., Tang, F. T., & Ju, C. W. (2001). Stress distribution of the foot during mid-stance to push-off in barefoot gait: a 3-D finite element analysis. *Clinical Biomechanics*, 16(7), 614–620. [https://doi.org/10.1016/s0268-0033\(01\)00047-x](https://doi.org/10.1016/s0268-0033(01)00047-x)
- Chen, Y. N., Chang, C. W., Li, C. T., Chang, C. H., & Lin, C. F. (2014). Finite Element Analysis of Plantar Fascia During Walking. *Foot & Ankle International*, 36(1), 90–97. <https://doi.org/10.1177/1071100714549189>
- Cheng, H., Liu, B., Liu, M., & Cao, W. (2022). Design of three-dimensional Voronoi strut midsoles driven by plantar pressure distribution. *Journal of Computational Design and Engineering*, 9(4), 1410–1429. <https://doi.org/10.1093/jcde/qwac060>
- Day, B. (2018, June 30). New survey reveals majority of Americans suffer from Foot Pain. New Survey Reveals Majority of Americans Suffer from Foot Pain. Retrieved October 30, 2022, from <https://www.prnewswire.com/news-releases/new-survey-reveals-majority-of-americans-suffer-from-foot-pain-259775741.html>
- Defrancesco, S., & Zanetti, V. (1983, November 1). Experiments on magnetic repulsion. *American Association of Physics Teachers*. <https://aapt.scitation.org/doi/10.1119/1.13365>
- Dr JK Ball of foot cushions — metatarsal pads, (n.d.). Retrieved November 14, 2022, from https://www.mliagestao.shop/index.php?main_page=product_info&products_id=300435
- DME for Less, metatarsal pads, (n.d.). Retrieved March 14, 2023, from <https://dmeforall.com/products/plantar-fasciitis-night-splint-pack>

- Engineers, L. M, (2022, October 29). Interface MPU6050 Accelerometer and Gyroscope Sensor with Arduino. Last Minute Engineers. <https://lastminuteengineers.com/mpu6050-accel-gyro-arduino-tutorial/>
- First for Magnets, (n.d.). Hazards Of Neodymium Magnets. <https://www.first4magnets.com/us/tech-centre-i1093/information-articles-i1401/neodymium-magnet-information-i1406/hazards-of-neodymium-magnets-i1417>
- Ice, (2022, November 15). The guide for MATLAB graph making. Zhihu. Retrieved March 13, 2023, from <https://zhuanlan.zhihu.com/p/583715105>
- Iqbal, M., Nauman, M. M., Khan, F. U., Abas, P. E., Cheok, Q., Iqbal, A., & Aissa, B, (2020). Multimodal Hybrid Piezoelectric-Electromagnetic Insole Energy Harvester Using PVDF Generators. *Electronics*, 9(4), 635. <https://doi.org/10.3390/electronics9040635>
- K&J Magnetics - Repelling Magnet Calculator, (n.d.). <https://www.kjmagnetics.com/calculator.repel.asp>
- Maleki, M, (2021, February 17). Interfacing CD74HC4067 16-Channel Multiplexer with Arduino. Electropeak. <https://electropeak.com/learn/interfacing-cd74hc4067-16-channel-analog-digital-multiplexer-with-arduino/>
- Mayo Foundation for Medical Education and Research, (2021, March 13). Foot pain causes. Mayo Clinic. Retrieved November 14, 2022, from <https://www.mayoclinic.org/symptoms/foot-pain/basics/causes/sym-20050792>
- Mayo Foundation for Medical Education and Research, (2022, January 20). Plantar fasciitis. Mayo Clinic. <https://www.mayoclinic.org/diseases-conditions/plantar-fasciitis/symptoms-causes/syc-20354846>
- Meng Chen, Bufu Huang, & Yangsheng Xu, (2008). Intelligent shoes for abnormal gait detection. *2008 IEEE International Conference on Robotics and Automation*. <https://doi.org/10.1109/robot.2008.4543503>
- Mirza, A., & McCrady, A, (2019, February 22). App Designer and Arduino. MATLAB Answers. Retrieved March 13, 2023, from <https://ww2.mathworks.cn/matlabcentral/answers/446098-app-designer-and-arduino>
- Nawoczenski, D. A., Birke, J. A., & Coleman, W, (1988). Effect of rocker sole design on plantar forefoot pressures. *Journal of the American Podiatric Medical Association*, 78(9), 455–460. <https://doi.org/10.7547/87507315-78-9-455>
- Orthopaedia, (n.d.). Anatomy, foot & ankle: Musculoskeletal medicine. <https://orthopaedia.com/page/Anatomy-of-the-Foot-Ankle>
- Tang, Y., Miao, R., Xie, X., Cao, J., Hu, Y., & Du, Z, (2020). Test and analysis on foot pain and discomfort pressure threshold in healthy adults. *China Leather*, 4. <https://doi.org/10.13536/j.cnki.issn1001-6813.2020-009-006>
- The safe distance of Neodymium Magnets*. Can magnets damage electric devices?, (n.d.). <https://www.supermagnete.de/eng/faq/What-is-the-safe-distance-that-I-need-to-keep-to-my-devices>
- Wagieh, A, (2019, June 14). Using Matlab app designer with Arduino. Instructables. Retrieved March 13, 2023, from <https://www.instructables.com/Using-MATLAB-App-Designer-With-Arduino/>
- Wei-Li, H., Xin-Xian, L., & Jiunn-Horng, K, (2005, July). Optimum position of metatarsal pad in metatarsalgia for pressure relief. *American journal of physical medicine & rehabilitation*. Retrieved November 14, 2022, from <https://pubmed.ncbi.nlm.nih.gov/15973088/>
- Wibowo, D. B., Suprihanto, A., Caesarendra, W., Glowacz, A., Harahap, R., Tadeusiewicz, R., Kańtoch, E., & Abas, P. E, (2021). A Design Study of Orthotic Shoe Based on Pain Pressure Measurement Using Algometer for Calcaneal Spur Patients. *Technologies*, 9(3), 62. <https://doi.org/10.3390/technologies9030062>
- Wikimedia Foundation, (2022, December 25). Halbach array. Wikipedia. Retrieved March 13, 2023, from https://en.wikipedia.org/wiki/Halbach_array
- Wikipedia contributors, (2022, December 7). Force between magnets. Wikipedia. https://en.wikipedia.org/wiki/Force_between_magnets
- Yaghoubi, H, (2012, September). Practical Applications of Magnetic Levitation Technology. maglev. http://www.maglev.ir/eng/documents/reports/IMT_R_22.pdf
- Yaghoubi, H, (2012, September). Practical Applications of Magnetic Levitation Technology. maglev. Retrieved November 1, 2022, from http://www.maglev.ir/eng/documents/reports/IMT_R_22.pdf
- Yang, J., & Yin, Y, (2020). Dependent-Gaussian-Process-Based Learning of Joint Torques Using Wearable Smart Shoes for Exoskeleton. *Sensors*, 20(13), 3685. <https://doi.org/10.3390/s20133685>

- Yang, J., & Yin, Y, (2021). Novel Soft Smart Shoes for Motion Intent Learning of Lower Limbs Using LSTM With a Convolutional Autoencoder. *IEEE Sensors Journal*, 21(2), 1906–1917. <https://doi.org/10.1109/jsen.2020.3019053>
- Yu, J., Cheung, J. T. M., Fan, Y., Zhang, Y., Leung, A. K. L., & Zhang, M, (2008). Development of a finite element model of female foot for high-heeled shoe design. *Clinical Biomechanics*, 23, S31–S38. <https://doi.org/10.1016/j.clinbiomech.2007.09.005>

Copyrights

Copyright for this article is retained by the author(s), with first publication rights granted to the journal.

This is an open-access article distributed under the terms and conditions of the Creative Commons Attribution license (<http://creativecommons.org/licenses/by/4.0/>).